Fuentes López, C.; Fuentes López, A.; Byrne, HJ.; Barat Baviera, JM.; Ruiz, MJ. (2022). In vitro toxicological evaluation of mesoporous silica microparticles functionalised with carvacrol and thymol. Food and Chemical Toxicology. 160:1-13. https://doi.org/10.1016/j.fct.2021.112778

In vitro toxicological evaluation of mesoporous silica microparticles functionalised with carvacrol and thymol

Cristina Fuentes[a1], Ana Fuentes[a], Hugh J. Byrne[b], José Manuel Barat[a], María José Ruiz[c]

[a]Department of Food Technology, Universitat Politècnica de València. Camino de Vera s/n, 46022, València, Spain

[b]FOCAS Research Institute, City Campus, Technological University Dublin, Dublin 8, Ireland

[c]Laboratory of Toxicology, Faculty of Pharmacy, Universitat de València, Av. Vicent Andrés Estellés s/n, 46100 Burjassot, Valencia, Spain

[1]**Corresponding author** Cristina Fuentes. Department of Food Technology, Universitat Politècnica de València. Camino de Vera s/n, 46022, Valencia, Spain: crifuelp@upvnet.upv.es

Abbreviations

ΔΨm, Mitochondrial membrane potential; APTES, (3-aminopropyl)triethoxysilane; BHT, di-ter-butyl- methylphenol; CTAB, Hexadecyltrimethylammonium bromide; DFA, Deferoxamine mesylate salt; DMEM, Dulbecco's Modified Eagle Medium; DMSO, Dimethyl sulfoxide; EOC, Essential oil component; H_2-DCFDA, 2′,7′-di-chlorodihydrofluorescein diacetate, IC_{50}, Mean inhibition concentration; LDH, Lactate dehydrogenase; LPO, Lipid peroxidation; MCM-41, Mobile composition of matter (MCM)-41; MDA, Malondialdehyde; MTT, Thiazolyl blue tetrazolium bromide; NBCS, Newborn calf serum; PBS, Phosphate buffered saline; PI, Propidium iodide; ROS, Reactive oxygen species; TBA, Thiobarbituric acid; TBARS, Thiobarbituric acid reactive substances; $TEAH_3$, Triethanolamine; TEM, Transmission electron microscopy

Abstract

The cytotoxicity of carvacrol- and thymol- functionalised mesoporous silica microparticles (MCM-41) was assessed in the human hepatocarcinoma cell line (HepG2). Cell viability, lactate dehydrogenase (LDH) activity, reactive oxygen species (ROS) production, mitochondrial membrane potential (ΔΨm), lipid peroxidation (LPO) and apoptosis/necrosis analyses were used as endpoints. The results showed that both materials induced cytotoxicity in a time- and concentration-dependent manner, and were more cytotoxic than free essential oil components and bare MCM-41. This effect was caused by cell-particle interactions and not by degradation products released to the culture media, as demonstrated in the extract dilution assays. LDH release was a less sensitive endpoint than the MTT (thiazolyl blue tetrazolium bromide) assay, which suggests the impairment of the mitochondrial function as the primary cytotoxic mechanism. *In vitro* tests on specialised cell functions showed that exposure to sublethal concentrations of these materials did not induce ROS formation during 2 h of exposure, but produced LPO and ΔΨm alterations in a concentration-dependent manner when cells were exposed for 24 h. The obtained results generally support the hypothesis that the carvacrol- and thymol-functionalised MCM-41 microparticles induced toxicity in HepG2 cells by an oxidative stress-related mechanism that resulted in apoptosis through the mitochondrial pathway.

Keywords: mesoporous microparticles; silica; essential oil components; cytotoxicity; HepG2

1. Introduction

Consumer awareness of additives and chemicals in their diets has forced the food industry to search for alternatives to synthetic preservatives to prolong their products' shelf life (Faleiro and Miguel, 2020; Ribes et al., 2018). In line with this, essential oils and their constituent components have attracted considerable attention for their natural origin and well-known antimicrobial and antioxidant activity (Burt, 2004; Hyldgaard et al., 2012). The monoterpenoids carvacrol and thymol, major components in essential oils from different plant species like origanum or thyme, are two of the most investigated essential oil components (EOCs) because of their marked action against a wide spectrum of foodborne and food spoilage microorganisms (Abbaszadeh et al., 2014; Abdelhamid and Yousef, 2021; Čabarkapa et al., 2019; Karam et al., 2019; Tippayatum and Chonhenchob, 2007; Walczak et al., 2021). These components' antimicrobial action has been attributed mainly to the presence of a hydroxyl group and a system of delocalised electrons in their chemical structure capable of disrupting the cytoplasmic membrane and leading to the leakage of intracellular content and, ultimately, lysis (Xu et al., 2008). However, their application to food products poses some challenges, such as high volatility, low solubility or strong sensory properties (Hyldgaard et al., 2012). Grafting EOCs onto the surface of silica particles has been proposed as a strategy to increase these components' antimicrobial activity and to overcome drawbacks. These hybrid organic-inorganic particles have efficiently performed as preservatives in different food matrices (Ribes et al., 2017, 2019) and as filtering materials for cold beverage pasteurisation (García-Ríos et al., 2018; Peña-Gómez et al., 2019a, 2019b, 2020).

Mobile composition of matter (MCM)-41 is one of the most widely employed scaffolds for the synthesis of organic-inorganic hybrid systems thanks to easy surface functionalisation, large surface area, uniform pore size and high stability (Diab et al.,

2017). Moreover, as a result of reported high biocompatibility and low toxicity (Aburawi et al., 2012; Al-Salam et al., 2011; Garrido-Cano et al., 2021), MCM-41 materials have been studied for the covalent attachment of functional groups and organic molecules in a number of oral applications (Bagheri et al., 2018; Ros-Lis et al., 2018). However, as the surface properties of particles are key factors for determining their interactions with biological systems (Kyriakidou et al., 2020; Puerari et al., 2019; Vicentini et al., 2017), the analysis of the *in vitro* and *in vivo* behaviours of surface-modified silica structures is crucial to guarantee the safety and innocuousness of their use for human health purposes.

Previous *in vitro* studies have evaluated the stability of different types of synthetic amorphous silica particles functionalised with carvacrol, eugenol and vanillin under conditions that represent the human gastrointestinal tract, lysosomal fluid and the cytotoxicity of these materials (Fuentes et al., 2021, 2020). The results showed that functionalisation with EOCs resulted in lower dissolution levels than bare MCM-41 microparticles and, therefore, increased stability under both biological conditions (Fuentes et al., 2020). Conversely, the comparative analysis of the cytotoxic effect of eugenol- and vanillin-functionalised silica particles revealed that free EOCs and bare particles had a milder cytotoxic effect on HepG2 cells than the functionalised MCM-41 materials. A relation between cytotoxicity and the density of EOC molecules on the surface of the functionalised particles was found. According to the physico-chemical analysis of the materials, properties like cationic nature and hydrophobicity were suggested to enhance the cytotoxic behaviour of the functionalised silica particles (Fuentes et al., 2021). All together, these results demonstrate that the functionalisation of MCM-41 particles with EOC derivatives enhances the stability of these materials under biological conditions, but may increase their cytotoxic behaviour that implies potential toxicological hazards. Besides, the molecular mechanism underlying these materials'

cytotoxic behaviour remains to be elucidated. Accordingly, with this work we aimed to investigate the cytotoxic effect of the carvacrol- and thymol-functionalised MCM-41 microparticles and to further elucidate the related toxicity mechanism. HepG2 cells were selected for the *in vitro* toxicology studies because this cell type is a standard model for xenobiotic metabolism and toxicity studies, and displays a high degree of reproducibility. Thus, HepG2 human liver cells were exposed to the modified silica materials, and then cell viability, lactate dehydrogenase (LDH) activity, reactive oxygen species (ROS) production, mitochondrial membrane potential ($\Delta\Psi m$), lipid peroxidation (LPO), and apoptotic and necrotic responses, were evaluated.

2. Materials and Methods

2.1. Reagents

Triethanolamine ($TEAH_3$), hexadecyltrimethylammonium bromide (CTAB), carvacrol (≥ 98% w/w), thymol (≥ 99% w/w), (3-aminopropyl) triethoxysilane (APTES), thiazolyl blue tetrazolium bromide (MTT), 2′,7′-di- chlorodihydrofluorescein diacetate (H_2-DCFDA), Rhodamine 123, thiobarbituric acid (TBA), deferoxamine mesylate salt (DFA) and di-ter-butyl- methylphenol (BHT) were obtained from Sigma-Aldrich (Spain). Dimethyl sulfoxide (DMSO) was purchased from Scharlab (Spain).

The HepG2 human hepatocarcinoma cell line was obtained from the American Type Culture collection (ATCC HB-8065). Dulbecco's Modified Eagle Medium (DMEM-Glutamax™) with high glucose (4.5 g/L), phosphate buffered saline (PBS), newborn calf serum (NBCS), penicillin, streptomycin, trypsin-EDTA 0.5% and sodium pyruvate were supplied by Gibco (Life-Technologies, USA).

2.2. Preparation of the EOCs-functionalised MCM-41 microparticles

106 The mesoporous silica microparticles MCM-41 were prepared via the 'atrane route'.
107 Under basic conditions, this is based on the use of $TEAH_3$, which generates atrane
108 complexes as inorganic hydrolytic precursors and CTAB as a structural directing agent
109 (Cabrera et al., 2000). The procedure of the synthetic process is fully described in Fuentes
110 et al. (2020).

111 Once synthesised, the functionalisation of the MCM-41 silica particles with carvacrol
112 and thymol was performed by a three-stage protocol that includes the: (1) synthesis of the
113 carvacrol and thymol aldehyde derivatives by direct formylation with paraformaldehyde;
114 (2) synthesis of the alkoxysilane derivatives by a reaction of carvacrol and thymol
115 aldehydes with APTES; (3) immobilisation of the alkoxysilane derivatives on the surface
116 of silica particles (García-Ríos et al., 2018).

117 **2.3. Physico-chemical characterisation of MCM-41 microparticles**

118 The bare and functionalised MCM-41 microparticles were analysed by transmission
119 electron microscopy (TEM), particle size distribution, zeta potential and the elemental
120 analysis. For the morphological analysis of the materials by TEM, particles were
121 dispersed in dichloromethane and sonicated for 2 min to avoid aggregation. The
122 suspension was placed on copper grids coated with a carbon film (Aname SL, Spain). The
123 imaging of the particle samples was done using a JEOL JEM-1010 (JEOL Europe SAS,
124 France) that operated at an acceleration voltage of 80 kV. The zeta potential of particles
125 was studied by laser Doppler microelectrophoresis using a Zetasizer Nano ZS (Malvern
126 Instruments, UK) and the Smoluchowski mathematical model. Particle size distribution
127 was determined by a laser diffractometer (Mastersizer 2000, Malvern Instruments, UK)
128 and applying the Mie theory (refractive index of 1.45, absorption index of 0.1). For the
129 zeta potential and the particle size distribution analysis, samples were measured in
130 triplicate on previously sonicated diluted dispersions in deionised water. Finally, the

elemental composition of the EOCs-functionalised particles was determined by a combustion analysis for C, H and N using a CHNS1100 Elemental Analyser (CE Instruments, UK).

2.4. Toxicological evaluation of the EOCs-functionalised MCM-41 microparticles

2.4.1. Cell culture

Human hepatocarcinoma (HepG2) cells were cultured in DMEM-Glutamax medium supplemented with 10% NBCS, 100 U/mL of penicillin and 100 μg/mL of streptomycin. Cells were maintained in a 5% CO_2 humidified incubator at 37 ºC. Growth medium was changed every 2–3 days or as required. Cells were subcultured by trypsinisation when about 80% confluence was reached and were used for experiments at passages between 9 and 24. Lack of mycoplasma contamination was examined regularly in cell cultures with the MycoAlert™ PLUS Myco-plasma kit (Lonza Rockland, USA).

2.4.2. Test solutions

Stock solutions of EOCs were prepared in DMSO (2.5 M) and were maintained at -20 ºC until used. Particle suspensions were prepared in the DMEM-supplemented medium and were sonicated for 10 min immediately before use. While studying the cytotoxic effect of carvacrol and thymol exposure, the final DMSO concentration in the test solutions was below 0.1%. Appropriate negative controls containing the same amount of solvents were included in each experiment. To analyse the MCM-41 materials, the cell-free particle control samples were included for each particle type and concentration, and were used to correct particle interference from test wells whenever necessary.

2.4.3. MTT assays

Direct exposure cytotoxicity assays

The MTT assay is one of the most widely used colorimetric assays to evaluate cell viability. In this method, the yellow positively charged tetrazolium salt enters viable cells, whereupon it is metabolically reduced to the insoluble blue-violet form of formazan by respiratory chain components (Rampersad, 2012). This assay was used to determine the mean inhibition concentration (IC_{50}) values of EOCs and the EOCs-functionalised silica, and to compare the cytotoxic effect of the functionalised particle constituents. Briefly, cells were seeded in 96-well plates at a density of 1 x 10^5 and 3 x 10^4 cells/mL for 24-hour and 48-hour experiments, respectively. After the 24-hour attachment, cells were exposed to serial dilutions of carvacrol (0.01-2.5 mM), thymol (0.06-1 mM), carvacrol- and thymol-functionalised MCM-41 microparticles (0.01-2.5 mg/mL) and to the equivalent concentrations of the EOCs, bare and functionalised particles for their comparative analysis (Table 1). The concentration ranges of EOCs and the functionalised particles were selected according to previous works (Fuentes et al., 2021). In the comparative studies, concentration ranges were established from the IC_{50} values found for carvacrol and thymol. Then the equivalent particle concentrations were calculated from the EOCs content determined by the elemental analysis. After a 24-hour or 48-hour incubation period, wells were washed with 100 µL of PBS. Next 100 µL of 10% MTT stock solution (5 mg/mL in PBS) in supplemented DMEM medium were added per well. Then plates were incubated in the dark at 37 ºC, 5% CO_2 for 3 h. Afterwards, the MTT solution was discarded, wells were washed with PBS and 100 µL of DMSO were added to dissolve formazan crystals. Finally, plates were shaken at 300 rpm for 10 min and absorbance was measured at 570 nm using a MultiSkan EX ELISA plate reader (Thermo Scientific, USA). Cell viability was expressed as a percentage in relation to the negative control (unexposed cells).

Exposure to sublethal concentrations of toxicants triggers the adaptative cellular responses linked with their cytotoxicity mechanism (Severin et al., 2017). For this reason, sublethal concentrations ($<IC_{50}$) were used to further investigate the toxicity mechanism underlying the exposure of the EOCs-functionalised particles. To this end, the IC_{50} values of the particles found in the MTT assay were used to calculate the sublethal concentrations ($IC_{50/2}$, $IC_{50/4}$, $IC_{50/8}$) for the different *in vitro* endpoints: ROS formation, $\Delta\Psi m$, LPO, and apoptotic and necrotic responses.

Table 1. Concentrations assayed in the comparative study of carvacrol, thymol, and bare and EOCs-functionalised MCM-41 microparticles.

	Concentrations			
	A	**B**	**C**	**D**
Carvacrol (mM)	0.25	0.5	1	2
Bare MCM-41 (mg/mL)	4.5	8.9	17.9	35.7
Carvacrol MCM-41 (mg/mL)	4.4	8.8	17.7	35.4
Thymol (mM)	0.25	0.5	1	2
Bare MCM-41 (mg/mL)	3.8	7.7	15.3	30.6
Thymol MCM-41 (mg/mL)	3.7	7.6	15.1	30.3

Extract exposure cytotoxicity assays

An extract dilution exposure method was applied to evaluate a possible cytotoxic effect due to the components leached from the surface of the functionalised particles to the culture medium. For this purpose, a stock solution of the carvacrol- or thymol-functionalised particles in the DMEM-supplemented medium (2.5 mg/mL) was vigorously stirred, sonicated in an ultrasonic bath for 10 min and maintained at 37 ^{o}C for 24 h. After this time, the stock solution was serially diluted (0.01-2.5 mg/mL) and

196 dilutions were filtered with 0.2 μm cellulose acetate filters to remove particles. Then cells
197 were exposed to the filtered solutions and samples' cytotoxicity was determined by the
198 MTT assay as described previously.

199 **2.4.4. Lactate dehydrogenase (LDH) activity**

200 LDH activity was determined by the CyQUANT LDH Cytotoxicity Assay kit (Thermo
201 Scientific, USA) according to the manufacturer's protocol. Briefly, cells were seeded in
202 96-well plates at 10^5 cells/mL (100 μL/well) and allowed to attach for 24 h. Then cells
203 were treated with 10 μL of the functionalised particle concentrations (0.01-2.5 mg/mL)
204 for a 24-hour period. Next 10 μL of sterile ultrapure water (Spontaneous LDH Activity)
205 or 10 μL of lysis buffer (Maximum LDH Release) were added to the control wells. Plates
206 were incubated in the dark at 37 °C and 5% CO_2 for 45 min. This was followed by
207 transferring 50 μL of each sample medium to a new plate and 50 μL of the reaction
208 mixture were incorporated. After incubation at room temperature for 30 min, reactions
209 were ended by adding 50 μL of the stop solution. Absorbance measurements were taken
210 in a microtiter plate reader at 490 nm. The results were expressed as LDH release (%) in
211 the exposed cells in relation to the spontaneous and maximum LDH controls.

212 **2.4.5. ROS formation**

213 ROS formation was determined as described by Ruiz-Leal and George (2004). Cells
214 were seeded in black 96-well microplates at 2×10^5 cells/mL density. After 24 h of cell
215 attachment, cells were washed with PBS and 20 μM of H_2-DCFDA dye in culture medium
216 were added. Following a 20-minute incubation time in the dark at room temperature, the
217 dye solution was removed and cells were exposed to different concentrations of the
218 functionalised particles (18.75, 37.5 and 75 μg/mL). Then fluorescence was measured
219 every 15 min for 2 h at 490 nm excitation and a 545 nm emission wavelength on a Wallace

220 Victor2, model 1420 multilabel counter (PerkinElmer, Finland). The ROS generation
221 percentage was expressed as the percentage of the fluorescence values obtained compared
222 to the negative control (unexposed cells).

223 **2.4.6. Determination of the mitochondrial membrane potential**

224 Mitochondrial membrane potential was determined by the uptake of green-fluorescent
225 dye Rhodamine 123 upon the exposure of the functionalised microparticles. Cells were
226 seeded at a density of 2×10^5 cells/mL in black 96-well microplates. After 24 h of cell
227 attachment, cells were washed with 100 µl/well PBS and were exposed to three different
228 concentrations of the functionalised particles (18.75, 37.5 and 75 µg/mL) in the 10%
229 NCBS-supplemented medium for 24 h. Following the exposure time, cells were washed
230 with 100 µl/well of PBS and Rhodamine-123 (5 µM) was added in the non-supplemented
231 medium. After 15 min of incubation at 37 ºC and 5% of CO_2 in the dark, the dye solution
232 was removed, and cells were washed twice and finally resuspended in 200 µl/well PBS.
233 Fluorescence (λexcitation=485 nm, λemission=535 nm) was measured using a microplate
234 reader Wallace Victor2, model 1420 multilabel counter (PerkinElmer, Finland). The
235 results were expressed as the fluorescence percentage of Rhodamine 123 dye in the
236 exposed cells compared to the negative control (unexposed cells).

237 **2.4.7. Lipid peroxidation assays**

238 The effect of sublethal concentrations' exposure to the functionalised particles upon
239 LPO was performed by determining the formation of thiobarbituric acid reactive
240 substances (TBARS) according to the method described by Ferrer et al. (2009). Briefly,
241 3×10^4 cells/well were seeded in 6-well plates, allowed to attach for 24 h and then
242 exposed to the functionalised particles (18.75, 37.5 and 75 µg/mL). After 24 h of
243 exposure, cells were washed with PBS, homogenised in 150 mM of sodium phosphate

buffer (NaH_2PO_4), pH 7.4, and lysate in the Ultra-Turrax T8 IKA®-WERKE for 30 s. Cell samples were mixed with 0.5% TBA, 1.5 mM of DFA and 3.75% BHT and heated at 100 ºC in a boiling water bath for 20 min. After cooling for 5 min, samples were centrifuged at 4,000 rpm for 15 min to remove the precipitate. The absorbance of the supernatant was then determined at 535 nm. Simultaneously, samples' protein content was measured following the Lowry method by the DC Protein Assay (BIO-RAD Laboratories, USA) at the 690 nm wavelength. The results were expressed as ng of malondialdehyde (MDA) per mg of protein.

2.4.8. Apoptosis/necrosis assays

The apoptosis/necrosis assays were performed by flow cytometry using the FITC Annexin V apoptosis detection kit (BD Biosciences, USA). Briefly, cells were seeded in 6-well plates at a density of 3 x 10^4 cells/well. After attachment, cells were exposed to the functionalised particles (18.75, 37.5 and 75 µg/mL) for 24 h. Then they were trypsinised, washed twice with ice-cold PBS and resuspended in binding buffer. A volume of cells of 100 µL (1 x 10^5 cells/mL) was stained by adding 5 µl of FITC Annexin V and 5 µl of propidium iodide (PI), which was incubated at room temperature in the dark for 15 min. After this time, 400 µL of binding buffer were added to each tube and samples were analysed in a BD LSRFortessa flow cytometer (BD Biosciensces, USA). Quadrant statistics were carried out to differentiate necrotic, early apoptotic and late apoptotic cells. The percentage of cells in each category was calculated by subtracting the number of cells in the control group from the number of cells in the treated population.

2.5. Statistical analysis

The statistical data analysis was performed using the Statgraphics Centurion XVI software package (Statpoint Technologies, Inc., USA). Data were expressed as the mean

(SEM) of three independent experiments for each endpoint. The data from the cytotoxicity assays were transferred to GraphPad Prism, version 8.0.1 (GraphPad Software, USA), to adjust the IC_{50} curve by using a four-parameter sigmoidal fit. The statistical analysis of the results was carried out by a Student's t-test for paired samples. In the MTT comparative study, differences between groups were analysed statistically by a one-way ANOVA, followed by the Tukey HDS *post-hoc* test for multiple comparisons. The difference level of $p \leq 0.05$ was considered statistically significant.

3. Results

3.1. Physico-chemical characterisation of the MCM-41 microparticles

To study the morphology and structure of the bare and carvacrol- or thymol-functionalised MCM-41 particles, a TEM analysis was performed. As shown in Figure 1, the three particle types exhibited an irregular external shape and a hexagonal periodic structure of internal channels in the form of alternate black and white parallel lines, typical of the ordered mesoporous structure of MCM-41 materials (Alothman, 2012; Meynen et al., 2009). These results confirmed that the synthesis process of the MCM-41 materials was correct and the functionalisation process did not significantly modify these materials' characteristic structure.

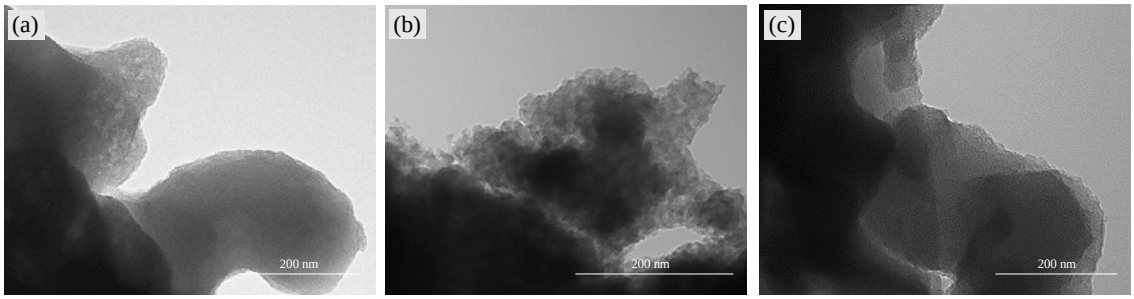

Figure 1. TEM images of the bare MCM-41 (a), carvacrol-functionalised MCM-41 (b) and thymol-functionalisedMCM-41 microparticles (c). Scale bar indicates 200 nm.

The zeta potential values and the particle size distribution of the bare and functionalised MCM-41 particles and the carvacrol or thymol contents of the MCM-41-functionalised materials are shown in Table 2. The negative zeta potential value observed for the bare MCM-41 was related to the negatively charged hydroxyl groups on the silica surface. In contrast, the functionalised particles displayed positive zeta potential values, which evidenced the presence of the carvacrol and thymol alkoxysilane derivatives grafted on their surface. Particle size distribution and TEM analysis showed that the three MCM-41 microparticles types were under 700 nm. This value was slightly higher for the bare than the functionalised particles as the larger number of steps included during the functionalisation process has been suggested to reduce the formation of agglomerates (Fuentes et al., 2020). Finally, the quantification of the carvacrol and thymol grafted onto particles' surface was determined by the elemental analysis. Small differences were found in the reaction yield for both types of EOCs, and the content of the thymol immobilised on the surface of the MCM-41 functionalised microparticles was slightly higher than carvacrol (Table 2). These results were used to establish the equal concentrations of the free EOCs and functionalised particles for the comparative cell viability assays (Table 1).

Table 2. Zeta potential (ZP) values, particle size distribution ($d_{0.5}$), particle size measured by TEM and EOC content (α) of the different MCM-41 microparticles.

Type of particle	ZP (mV)	$d_{0.5}$ (μm)	Size (μm)	α (g/gSiO_2)
Bare MCM-41	-33.43 (0.84)	0.68 (0.00)	0.63 (0.4)	
Carvacrol-MCM-41	27.37 (2.06)	0.62 (0.00)	0.57 (0.3)	0.0084
Thymol-MCM-41	21.07 (1.74)	0.65 (0.00)	0.50 (0.6)	0.0098

ZP and $d_{0.5}$ values are expressed as mean (SD) (n=3).

3.2. Toxicological evaluation of the EOCs-functionalised MCM-41 microparticles

3.2.1. MTT assays

Firstly, the cytotoxic effect of carvacrol and thymol was determined after the 24 h and 48 h exposures of HepG2 cells, as determined by the MTT assay. Both components reduced cell viability in a time- and concentration-dependent manner (Figs. S1 and S2). Carvacrol was slightly less cytotoxic than thymol when cells were exposed to EOCs for 24 h. However, no differences were found after the 48-hour incubation period. The IC_{50} values obtained after 24 h exposure were 0.45 (0.01) mM and 0.40 (0.03) mM for carvacrol and thymol, respectively. At 48 h, the IC_{50} value for both components was similar: (0.32 (0.02) mM for carvacrol and 0.32 (0.03) mM for thymol).

Figure 2 displays the cytotoxicity-response curves for the carvacrol- and thymol-functionalised MCM-41, added either directly to the culture medium or in an extract dilution form. Both materials reduced cell viability in a concentration-dependent manner (Fig. S3) when HepG2 cells were directly exposed to the functionalised particles for 24 h and 48 h, as measured by the MTT assay. The IC_{50} values obtained for the carvacrol-functionalised MCM-41 were 0.15 (0.01) mg/mL and 0.09 (0.04) mg/mL for 24 h and 48

h, respectively. The thymol-functionalised microparticles gave an IC_{50} value of 0.15 (0.08) mg/mL after a 24-hour cell exposure and 0.11 (0.08) mg/mL after 48 h. However, when cells were treated with the filtered medium which previously contained each particle type, cell viability was significantly higher. A cell viability of 75% and 78% for the carvacrol- and thymol-functionalised silica was, respectively, observed after 24 h of exposure to the highest tested concentrations (2.5 mg/mL). After 48 h of treatment, these percentages were 92% for the carvacrol-functionalised particles and 85% for the thymol-functionalised silica. When cells were exposed to the filtered solutions equivalent to the IC_{50} values obtained for both functionalised particle types, cell viability remained around 100%.

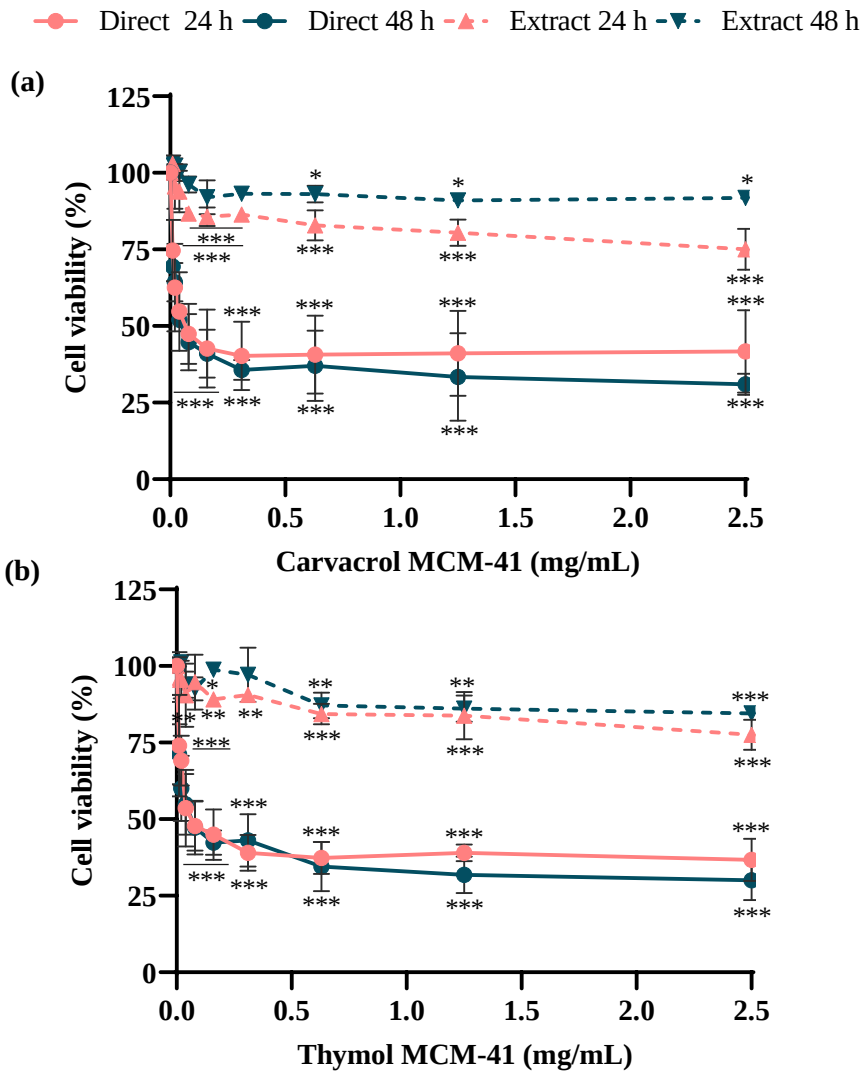

339

340 **Figure 2.** Concentration-cell viability plots of the HepG2 cells exposed either directly
341 or in an extract dilution form to the carvacrol-functionalised MCM-41 (a); and the
342 thymol-functionalised MCM-41 (b) for 24 h and 48 h by the MTT assay. Each bar
343 represents the mean (SEM) of three independent assays, each performed 6-fold. (*) $p \leq$
344 0.05; (**) $p \leq 0.01$; (***) $p \leq 0.001$ indicates significant differences compared to the
345 control according to the Student's t-test.

346

347 The IC_{50} values previously found for carvacrol and thymol were used to define the
348 concentration range for the comparative analysis of the cytotoxic effects of the free EOCs,

EOC-functionalised MCM-41 and bare MCM-41 microparticles. The results of the comparative analysis are shown in Figure 3. Free carvacrol was significantly less cytotoxic than the equivalent concentrations of carvacrol anchored to the surface of silica microparticles at the two lowest assayed concentrations (0.25 and 0.5 mM). Differences in cell viability between the free carvacrol and carvacrol-functionalised MCM-41 ranged from 75% to 32% and from 61% to 24% after 24 h and 48 h exposure, respectively. The bare MCM-41 microparticles also showed a lower cytotoxic response than the equivalent concentrations of the functionalised materials at the three highest concentrations tested for both exposure times. Differences in cell viability between the bare MCM-41 and carvacrol-functionalised MCM-41 ranged from 75% to 47% and from 89% to 47% after treating cells for 24 h and 48 h, respectively.

For thymol, the free compound was significantly less cytotoxic than the equivalent concentration of the immobilised compound on the MCM-41 microparticles at the highest tested concentration (0.25 mM). At this concentration, the differences in cell viability between the free thymol and thymol-functionalised MCM-41 were 59% and 61% after 24 h and 48 h exposure, respectively. The bare MCM-41 was less cytotoxic than the thymol-functionalised MCM-41 at the 0.25 mM and 0.5 mM concentrations. At these concentrations, the differences in cell viability between both particle types ranged from 65% to 44% and from 61% to 55% after 24 h and 48 h exposure, respectively.

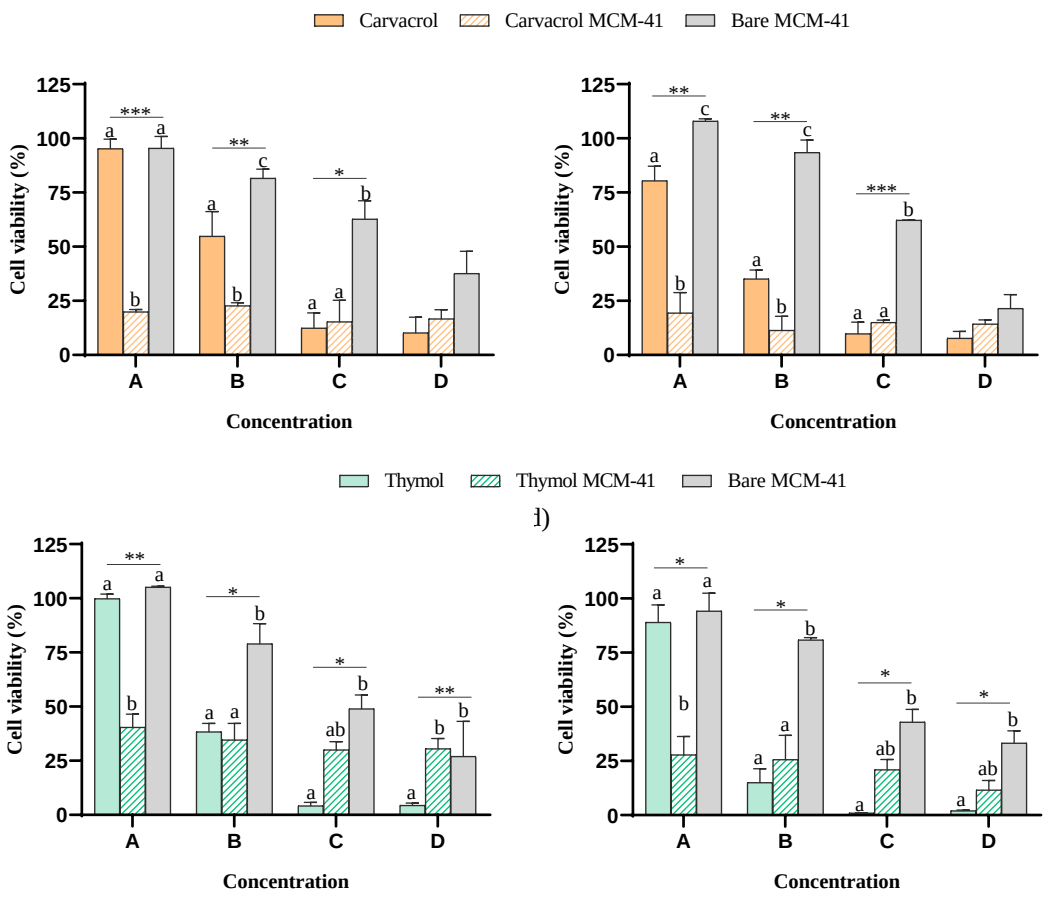

Figure 3. Concentration-cell viability plots of the HepG2 cells exposed to the equivalent concentrations of carvacrol-, the carvacrol-functionalised MCM-41 and the bare MCM-41 for 24 h (a) and 48 h (b) or to the equivalent concentrations of thymol, the thymol-functionalised MCM-41 and the bare MCM-41 for 24 h (c) and 48 h (d). Each bar represents the mean (SEM) of three independent assays, each performed 6-fold. Significant differences (***p ≤ 0.01, **p ≤ 0.01, *p ≤ 0.05) are indicated by different letters (a–c).

3.2.2. LDH assay

The LDH assay measures the activity of LDH released in cell culture medium after exposure to cytotoxic substances. It is an indicator of irreversible cell death due to cell

membrane damage (Aslantürk, 2018). Therefore, higher LDH values in the medium indicate higher toxicity levels. Figure 4 depicts the effect of the EOCs-functionalised particles on LDH release to the medium after 24 h of exposure. As this figure illustrates, the carvacrol- and thymol-functionalised silica exposures resulted in a significant increase in LDH release compared to the controls at the highest tested concentrations. Exposure to 2.5 mg/mL of the carvacrol-functionalised silica increased the LDH release by more than 10% compared to the control. For the thymol-functionalised silica at the two highest tested concentrations (1.25 and 2.5 mg/mL), LDH leakage into the culture medium increased by 14% and 16%, respectively. No differences were observed at all the other tested concentrations compared to the control.

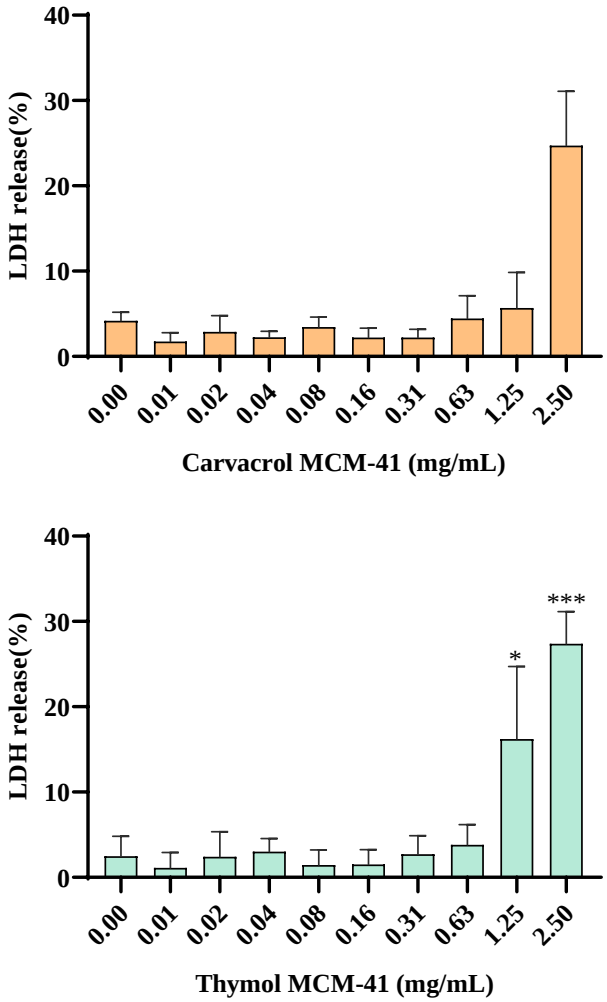

Figure 4. LDH activity in the HepG2 cells exposed to the carvacrol-functionalised MCM-41 microparticles (a) and the thymol-functionalised MCM-41 microparticles (b) for 24 h. The results are expressed as the mean (SEM, n=3). (*) $p \leq 0.05$; (**) $p \leq 0.01$; (***) $p \leq 0.001$ indicates significant differences compared to the control according to the Student's t-test.

3.2.3. ROS formation

ROS formation was studied as an indicator of oxidative stress using fluorescein derivative H_2DCF-DA. Figure 5 shows ROS production on the HepG2 cells exposed to

18.75, 37.5 and 75 µg/mL of the carvacrol- and thymol- functionalised MCM-41 microparticles after 120 min of postexposure. As shown, exposure to the three concentrations of both the functionalised particle types did not induce ROS formation over this time period as no significant differences in DCFDA dye fluorescence intensity were observed compared to the control cells.

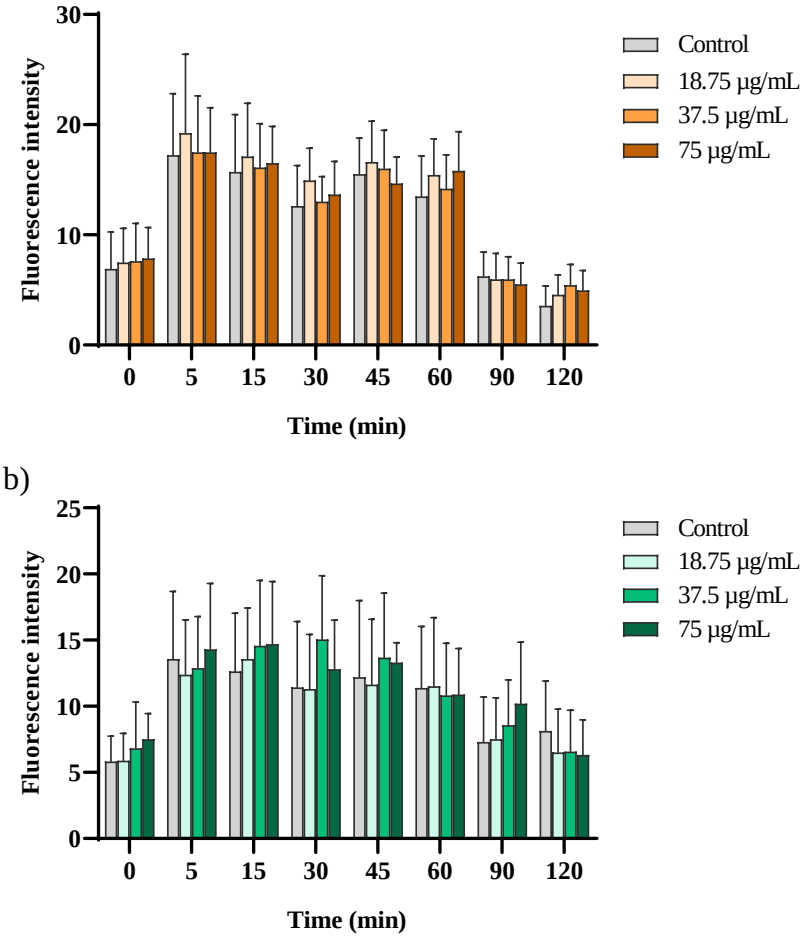

Figure 5. ROS induction according to time (0-120 min) in the HepG2 cells exposed to the sublethal concentrations of the carvacrol-functionalised MCM-41 microparticles (a) and thymol-functionalised MCM-41 microparticles (b). The results are expressed as the mean (SEM, n=3). No significant differences were found between the different test solutions and the control.

3.2.4. Lipid peroxidation assays

The MDA levels were measured as an indicator of LPO and oxidative stress by the TBARS assay. LPO production on HepG2 cells in the presence of the carvacrol- and thymol-functionalised silica at 18.75, 37.5 and 75 μg/mL is observed in Figure 6. The obtained results demonstrated that 24 h of exposure to the carvacrol-functionalised particles significantly increased MDA production by 44% (18.75 μg/mL), 15% (37.5 μg/mL) and 54% (75 μg/mL) in relation to the control cells. Similarly, 24 h of exposure to the thymol-functionalised particles significantly increased MDA levels in a concentration-dependent manner (Fig. 6). Exposure to 18.75, 37.5 and 75 μg/mL of the thymol-functionalised MCM-41 for 24 h resulted in an increase of 17%, 24% and 55%, respectively, compared to the control.

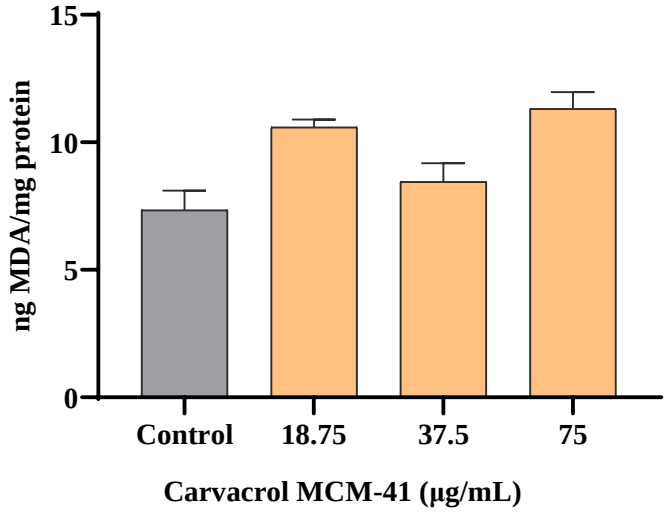

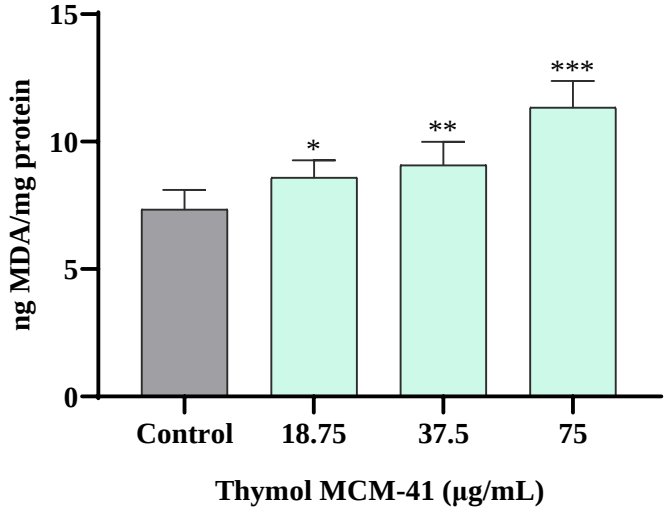

424

425 **Figure 6.** Effect on LPO as measured by MDA production after HepG2 cells exposure to
426 sublethal concentrations of the carvacrol-functionalised MCM-41 microparticles (a) and
427 thymol-functionalised MCM-41 microparticles (b) for 24 h. The results are expressed as
428 the mean (SEM, n=3). (*) $p \leq 0.05$; (**) $p \leq 0.01$; (***) $p \leq 0.001$ indicates significant
429 differences compared to the control according to the Student's t-test.

430

431 **3.2.5. ΔΨm determination**

To assess whether the exposure of the functionalised particles affected mitochondrial function, potential changes in ΔΨm were analysed by employing mitochondria fluorescent dye Rhodamine 123. As shown in Figure 7, 24 h of exposure to both materials induced a significant drop in ΔΨm in a concentration-dependent manner. This effect was stronger for the carvacrol-functionalised particles that decreased ΔΨm at the two highest tested concentrations (37.5 µg/mL and 75 µg/mL) by 19% and 28% in relation to the control, respectively. The thymol-functionalised particles at the 75 µg/mL concentration resulted in a significant 24% decrease in ΔΨm compared to the untreated control cells.

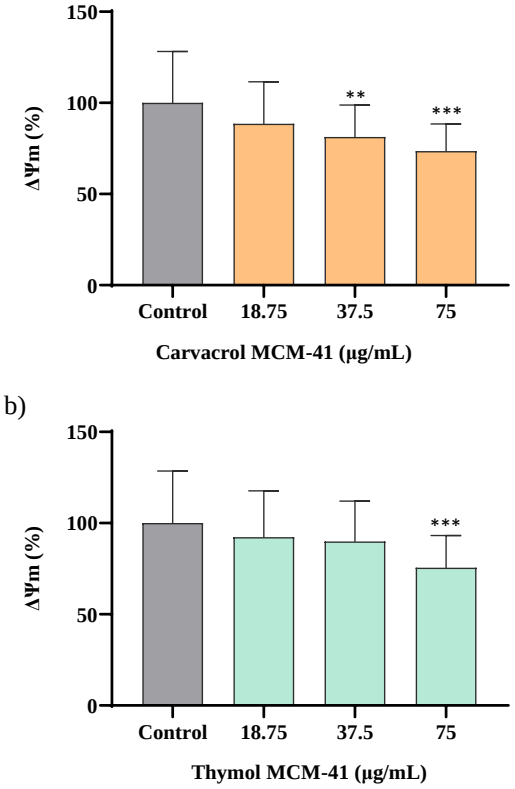

Figure 7. Effect on mitochondrial membrane potential (ΔΨm) after HepG2 cells' exposure to sublethal concentrations of the carvacrol-functionalised MCM-41 microparticles (a) and thymol-functionalised MCM-41 microparticles (b) for 24 h. The results are expressed as the mean (SEM, n=3). (**) $p \leq 0.01$; (***) $p \leq 0.001$ indicates significant differences compared to the control according to the Student's t-test.

3.2.6. Apoptosis and necrosis assays

The flow cytometry analysis was applied to determine the related death mechanism underlying the cytotoxic effect observed for the functionalised materials. Fluorescein Annexin V-FITC/PI double staining was used to distinguish and quantify the percentage of the necrotic, early apoptotic and late apoptotic cells after exposure to sublethal concentrations of the carvacrol- and thymol-functionalised MCM-41 (Fig. 8 and Fig. 9, respectively). The results revealed an increase in the percentage of the necrotic, early apoptotic and late apoptotic cells following treatment with rising concentrations of both the functionalised particles. However, significant differences were found only between the control cells and the cells exposed to the highest tested concentrations of both materials (75 µg/mL). The basal necrotic population in the control was 2.76 (0.40) %. After the treatment with 75 µg/mL of the carvacrol- and thymol-functionalised particles for 24 h, the necrotic rate rose to 10.20 (3.82) % and 8.63 (3.54) %, respectively. The percentage of the early apoptotic HepG2 cells increased from 6.65 (1.73) % in the unexposed control cells to 15.90 (3.46) % and 13.31 (1.83) % for the carvacrol- and thymol-functionalised MCM-41, and in this order. Similarly, the percentage of the late apoptotic cells went from 8.16 (0.26) % in the untreated culture to 16.27 (0.20) % and 13.98 (2.18) % for the carvacrol- and thymol-functionalised particles' exposed cells, respectively.

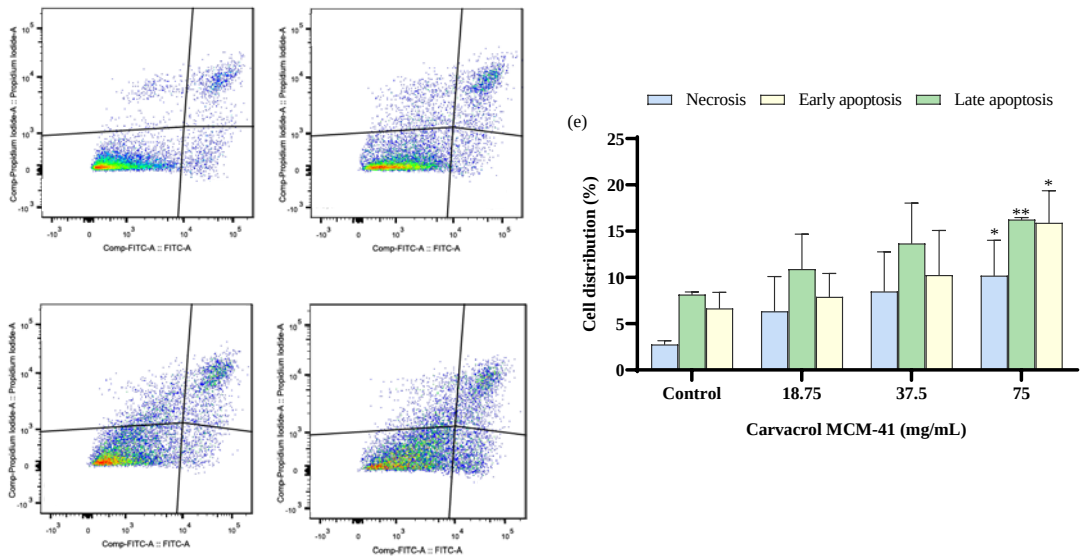

Figure 8. Flow cytometry analysis of the apoptotic and necrotic HepG2 cells exposed to sublethal concentrations of the carvacrol-functionalised MCM-41 microparticles using Annexin V-FITC/PI double staining. Representative two-dimensional dot plot diagrams of three independent experiments for: (a) the untreated cells; (b) the cells treated with 18.75 µg/mL; (c) 37.5 µg/mL; (d) 75 µg/mL of the carvacrol-functionalised MCM-41 microparticles. The upper left quadrant (PI+/Annexin V-FITC-) represents the necrotic cells, the left lower quadrant (PI-/Annexin V-FITC-) depicts the live cells, the upper right quadrant (PI+ /Annexin V-FITC+) refers to the late apoptotic cells and the lower right quadrant (PI-/Annexin V-FITC+) represents the early apoptotic cells. (e) The percentage of the early apoptotic, late apoptotic and necrotic cells. The results are expressed as the mean (SEM, n=3). (*) $p \leq 0.05$; (**) $p \leq 0.01$ indicates a significant difference compared to the control according to the Student's t-test.

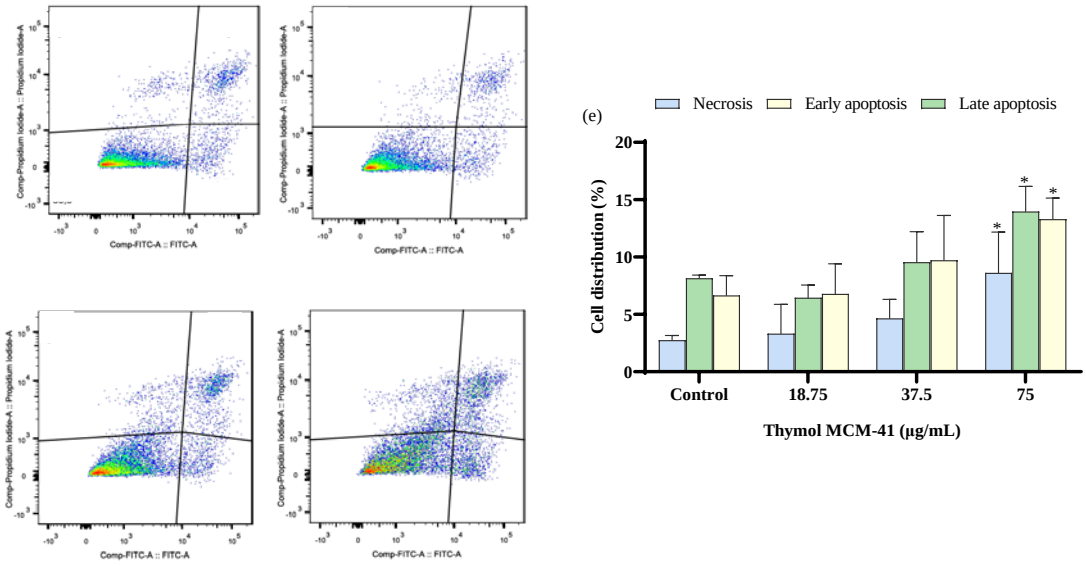

Figure 9. Flow cytometry analysis of the apoptotic and necrotic HepG2 cells exposed to sublethal concentrations of the thymol-functionalised MCM-41 microparticles using Annexin V-FITC/PI double staining. Representative two-dimensional dot plot diagrams of three independent experiments for: (a) the untreated cells; (b) the cells treated with 18.75 µg/mL; (c) 37.5 µg/mL; (d) 75 µg/mL of the thymol-functionalised MCM-41 microparticles. The upper left quadrant (PI+/Annexin V-FITC-) represents the necrotic cells, the left lower quadrant (PI-/Annexin V-FITC-) denotes the live cells, the upper right quadrant (PI+ /Annexin V-FITC+) refers to the late apoptotic cells and the lower right quadrant (PI-/Annexin V-FITC+) represents the early apoptotic cells. (e) The percentage of the early apoptotic, late apoptotic and necrotic cells. The results are expressed as the mean (SEM, n=3). (*) $p \leq 0.05$ indicates a significant difference compared to the control according to the Student's t-test.

4. Discussion

The immobilisation of natural EOCs on the surface of silica particles has emerged as an innovative technology to enhance their antimicrobial and antioxidant properties.

However, their safety needs to be addressed given their possible application to food or food contact materials. For this purpose, the potential health hazards that derive from exposure to these new materials for consumer health should be thoroughly investigated at the cellular level. The use of cell cultures is a relevant tool in toxicity testing to improve our understanding of hazardous materials and to predict their effects on human health (Eisenbrand et al., 2002). Assays that determine basal cytotoxicity measure cell viability or cell death as a consequence of damage to basic cellular functions, and allow the rapid identification of toxic compounds. Moreover, *in vitro* tests of specialised cell functions and metabolic endpoints provide insight into the pathways and mechanisms of action involved in chemically induced toxicity at both the molecular and cellular levels. This study examines the *in vitro* toxic effect of the carvacrol- and thymol-functionalised MCM-41 silica particles on HepG2 cells as a model cell line. The aim was to evaluate their potential toxicity and to fully understand the associated involved mechanism.

Firstly, a comparative analysis of the functionalised-particles and their constituents was carried out. It revealed that the free EOCs and bare MCM-41 microparticles exhibited significantly milder cytotoxic effects than the equivalent EOC-functionalised silica concentrations. Similar results have been found for eugenol- and vanillin-functionalised MCM-41 microparticles (Fuentes et al., 2021). In that study, the stronger cytotoxic effect observed for the EOCs-functionalised silica was attributed to physico-chemical properties, such as surface charge and hydrophobicity, which could be responsible for promoting interactions of EOCs with cell membranes. Previous studies have demonstrated that surface functionalisation may enhance the toxicity of silica particles (Dumitrescu et al., 2017; Paatero et al., 2017; Puerari et al., 2021; Yu et al., 2011). Chen et al. (2009) indicated that functionalisation with carvacrol increased the cytotoxicity of chitosan nanoparticles in a 3T3 mouse fibroblast cell line. The IC_{50} value observed for

carvacrol-grafted chitosan nanoparticles was around 1 mg/mL, whereas cell viability was still higher than 80% at the 2 mg/mL concentration of the unmodified chitosan nanoparticles as measured by the MTT assay. However, carvacrol-modified chitosan nanoparticles were significantly less cytotoxic to mammalian cells than free carvacrol. As previously reported, this discrepancy may be the result of differences in the starting material, the cell type employed for the cytotoxicity assays or the lower degree of grafting achieved for silica particles (Fuentes et al., 2021).

Cytotoxicity data may serve to predict acute systemic toxicity *in vivo* and to also define the concentration range for mechanistic toxicity studies (Ciappellano et al., 2016; Severin et al., 2017). With this 2-fold objective, the cytotoxicity of the carvacrol- and thymol-functionalised microparticles was analysed by two methods based on different physiological endpoints; the MTT and the LDH release assays. As measured by the MTT method, 24 h of exposure gave an IC_{50} value of 0.15 mg/mL for both the functionalised materials, and this value lowered to 0.09 mg/mL and 0.11 mg/mL after the 48-hour treatment, for carvacrol- and thymol-silica, respectively. In a previous work, Fuentes et al., 2021 determined the cytotoxic effect of bare MCM-41 silica microparticles on HepG2 cells by the MTT assay and confirmed the biocompatibility reported for calcined mesoporous silica (Aburawi et al., 2012; Al-Salam et al., 2011; Samri et al., 2012; Shamsi et al., 2010). Exposing cells to bare MCM-41 silica for 24 h and 48 h led to IC_{50} values of 18.90 mg/mL and 15.82 mg/mL, respectively (Fuentes et al., 2021). In comparison to these results, we found herein that the functionalisation of MCM-41 microparticles with carvacrol or thymol increased the cytotoxicity of the starting material by approximately 100-fold. However, when cells were exposed to the filtered medium which previously contained the particles during the extract dilution assays, cell viability remained at around 100% at the IC_{50} values calculated for both materials. These results can be interpreted as

a confirmation of a direct interaction of cells with particles that is responsible for the cytotoxic behaviour found for both the carvacrol- and thymol-functionalised particles; while an indirect cytotoxicity effect due to components leached from the functionalised particles' surface or by the depletion of nutrients from the culture medium (Casey et al., 2008) is not expected.

The cytotoxic effects assessed by the LDH assay were observed at higher particle concentrations than with the MTT assay and, thus, demonstrates that the MTT assay was more sensitive than the LDH assay for determining cell viability after the exposure of the EOCs-functionalised microparticles. The sensitivity of the different cytotoxicity assays differs depending on the mechanisms leading to cell death (Weyermann et al., 2005). The MTT method determines mitochondrial metabolic activity of viable cells, while the LDH assay measures cell death due to cell membrane damage. Hence concerning their sensitivity, the differences observed between both assays may suggest that impairment of the mitochondrial function may precede the disruption of membrane integrity and cell lysis in cells exposed to the carvacrol- and thymol-functionalised microparticles. Moreover, these results support the widespread consensus than more than one cell viability assay should be used to increase the reliability of the results during *in vitro* studies (Aslantürk, 2018; Eisenbrand et al., 2002; Fotakis and Timbrell, 2006).

It is worth mentioning that different studies have described particle interference when testing cytotoxicity with both methods (Holder et al., 2012; Kroll et al., 2012). Distinct factors have been proven to limit the sensitivity of the MTT method, including pH, optical activity or surface reactivity of particles (Abbasi et al., 2021; Laaksonen et al., 2007). In the LDH assay, different inorganic particles have been demonstrated to interfere with this assay by either adsorbing or inactivating the LDH protein, and both mechanisms involve decreased absorbance in the LDH assay that results in a false indication of a non-toxic

response (Holder et al., 2012). Korhonen et al. (2016) used the LDH assay to evaluate the cytotoxic effect of mesoporous silica microparticles on human corneal epithelial (HCE) and retinal pigment epithelial (ARPE-19) cells. These authors found increased or decreased reactivity in the LDH assay depending on the employed cell culture medium. Herein the MTT and LDH viability assays were also performed under cell-free conditions to evaluate any interference of the functionalised particles with both assays. At low concentrations, the EOCs-functionalised materials did not induce any non-specific response in the MTT and LDH viability assays. At concentrations higher than 0.31 mg/mL of particles, significantly increased absorbance was observed for both the cell-free assays. Consequently, data were corrected to avoid any particle interferences by subtracting the absorbance of the cell-free controls from that of the test wells.

In order to gain insight into the cytotoxicity mechanism induced by these materials, different endpoints related to oxidative stress, mitochondrial dysfunction and the cell death pathway were investigated. In this aspect of the work, the IC_{50} values for both materials obtained by the MTT assay were used to define the concentration range for further assays.

Oxidative stress is a major mechanism involved in the toxicity induced by many xenobiotics (Zhang, 2018). It results from an imbalance between the production of oxidising molecular species and the protective mechanisms produced by cells for their removal. Under normal conditions, ROS are oxygen-containing chemically-reactive molecules are produced by cells as a consequence of aerobic metabolism (Ray et al., 2012). However, the overproduction and accumulation of ROS due to interactions of cells with toxic agents may lead to an antioxidant system dysfunction, and also to oxidative damage to cellular macromolecules like lipids, proteins or nucleic acids, which causes severe cell toxicity (Eisenbrand et al., 2002). To evaluate whether oxidative stress was

involved in carvacrol- and thymol-functionalised MCM-41 cytotoxicity, two different biomarkers were used: ROS production and LPO generation. The results showed that exposure to the sublethal concentrations of both materials did not induce early ROS formation as measured by the DCFDA assay. However, the MDA levels significantly increased when cells were exposed to particles for 24 h, which indicates that oxidative stress occurred through LPO.

High ROS levels that persist for a long period are thought to be the major factor responsible for reacting with polyunsaturated fatty acids of lipid membranes and for inducing LPO (Barrera, 2012). Lack of ROS in this study may be explained by the differences in the exposure times employed between both assays. ROS formation was measured within 2 hour after exposure to the sublethal functionalised silica concentrations, while LPO was determined when cells were treated with these materials for 24 h. Accordingly, Santos et al. (2010) evaluated ROS production following exposure to different mesoporous silicon microparticles in human colon carcinoma Caco-2 cell line by the DCFDA assay. These authors found no significant increases in hydrogen peroxide concentrations or mitochondrial superoxide after a 3-hour incubation time, but observed a significant increase in hydrogen peroxide formation after 24 h exposure. Longer exposure times than those usually employed by this method have also been necessary to detect oxidative stress caused by other toxic insults (Aranda et al., 2013). Some authors also suggest that, although the DCFDA probe has been extensively employed as a biomarker of oxidative stress and is assumed to reflect the overall oxidative status of cells, it can only detect hydrogen peroxides, peroxyl radicals and peroxynitrite anions, and not all the different ROS types (Herzog et al., 2009).

Toxic agents can generate ROS by directly interacting with the electron-transport chain complexes in the inner mitochondrial membrane (Boelsterli, 2007). Moreover, cell-

622 particle interactions can induce ROS formation by a surface-catalysed reaction (Lehman
623 et al., 2016). Indeed silica particles have been demonstrated to induce ROS formation by
624 both mechanisms; direct contact of the cell membrane with particles' surface and by
625 triggering cell-signalling pathways that initiate cytokine release and apoptosis within cells
626 (Hamilton et al., 2008). Different phenomena, including hydrophobic or hydrophilic
627 interactions, active electron configurations, redox potential or semiconductor and
628 electronic properties, may be responsible for ROS generation upon the interactions of
629 particles with biological systems (Santos et al., 2010). In line with this, Lehman et al.
630 (2016) studied the free radical species generated from the surface of non-porous and
631 mesoporous nanoparticles by electron paramagnetic resonance spectroscopy. These
632 authors found a correlation between the ROS released from the nanoparticle surface,
633 intracellular ROS and cellular toxicity in murine macrophage cell line RAW 264.7.
634 Moreover, amine-functionalisation reduced the amount of the free radical generated at
635 the solid–liquid interface by non-porous nanosilica and, as suggested by the authors, this
636 would mitigate their toxic behaviour. Similarly, Santos et al. (2010) found surface
637 chemistry to be a determinant factor that establishes ROS production and cell-particle
638 interactions. According to their work, thermally carbonised particles induced toxicity as
639 a result of stimulating ROS production on Caco-2 cells, while thermally oxidised particles
640 did not induce significant ROS formation and resulted in less cell damage as a result of
641 weak cell-particle interactions. In our work, the increased cytotoxicity found for the
642 EOCs-functionalised compared to the native microparticles may be attributed to
643 differences in the surface properties between the bare and EOCs-functionalised particles.
644 Cationic nature and hydrophobic surfaces have been demonstrated to increase *in vitro*
645 toxicity and the number of apoptotic cells as a result of strong cell-particle interactions

(Saei et al., 2017; Santos et al., 2010). These properties may, therefore, be related to the increased cytotoxicity found for the functionalised materials in our study.

A close relation exists between ROS formation and mitochondria as these organelles are considered the main source of ROS in the cell. At the same time, mitochondrial damage by ROS formation is a main mechanism of toxicant-induced cytotoxicity (Zhang, 2018). Accordingly, mitochondrial dysfunction is one of the most sensitive indicators of adverse cell effects that can be evaluated by monitoring changes in $\Delta\Psi m$ of exposed cells (Xu et al., 2004). In this study, $\Delta\Psi m$ depletion was observed after treating HepG2 cells with the carvacrol- and thymol-functionalised silica. The generated $\Delta\Psi m$ is an essential component within a range of processes, including energy storage during oxidative phosphorylation, calcium homeostasis or cellular differentiation. Moreover, mitochondrial integrity disruption has been described as one of the early events that lead to apoptosis and may serve as a biomarker for apoptotic cell death (Jeong and Seol, 2008).

Exposure to cytotoxic agents can lead to cell death mainly by two major mechanisms: apoptosis and necrosis. In this work, the death mechanism related to the cytotoxic effects induced by modified-MCM-41 exposure was evaluated using the Annexin V-FITC/PI double staining and flow cytometry analysis. This method allows healthy, early apoptotic, late apoptotic and necrotic cells to be discriminated. We found that all three early apoptotic, late apoptotic and necrotic rates significantly rose after treating HepG2 cells at the highest sublethal concentration of both the carvacrol- and thymol-functionalised silica for 24 h. According to these results, both mechanisms of cell death are involved in the cytotoxicity induced by the EOCs-functionalised MCM-41.

Apoptosis, or programmed cell death, is a slow form of cell death that can occur under normal physiological conditions or may be induced by apoptotic compounds. There are two main pathways that lead to apoptosis: the extrinsic or death-receptor pathway, which

is activated from outside the cell by the ligation of transmembrane death receptors; the intrinsic or mitochondrial pathway, which begins with the permeabilisation of the mitochondrial outer membrane triggered by different signals, such as DNA damage, ischaemia or oxidative stress (Wang and Youle, 2009). ΔΨm depletion brings about the release of mitochondrial intermembrane space proteins to the cytoplasm, including cytochrome c, which consequently triggers other apoptotic factors, such as caspases activation or chromosome fragmentation, to lead to apoptosis through the mitochondrial or intrinsic pathway apoptotic death pathway (Tait and Green, 2013). Therefore, loss of ΔΨm serves as a biomarker of apoptotic cell death.

Unlike apoptosis, necrosis consists in a rapid cell death form that is induced by external injuries, such as hypothermia, radiation, hypoxia or chemicals that damage the cell membrane (D'Arcy, 2019). Destruction of the plasma membrane or the biochemical supports of its integrity leads to the release of intracellular material, local inflammatory responses, cell swell and lysis (Miret et al., 2006). Consequently, necrosis can be measured by the presence of the cytoplasmic content in extracellular fluid i.e. by measuring the activity of enzymes like LDH. As previously explained, the LDH assay was far less sensitive that the MTT assay for evaluating the basal cytotoxicity on HepG2 cells as a result of microparticles' exposure, and suggests impairment of mitochondrial activity rather than cell membrane disruption. As a result, we hypothesise that apoptosis is the most likely mechanism of cell death after the exposure of the EOCs-functionalised particles.

According to our results, the mechanism underlying the cytotoxic effect of the carvacrol- and thymol-functionalised silica microparticles on HepG2 cells involves oxidative stress induction, which will cause mitochondrial dysfunction and lead to apoptotic death pathway activation. This mechanism of toxic action bears similarities with the mechanism

696 described for their constituents. Essential oils and their components have been
697 demonstrated to induce toxicity in eukaryotic cells due to a phenolic-like prooxidant
698 mechanism (Bakkali et al., 2008). These components penetrate cells and permeabilise
699 cytoplasmic, and especially, mitochondrial membranes. Then damaged mitochondria
700 produce ROS by generating reactive phenoxyl radicals with a pro-oxidant potential that
701 may oxidise EOCs. Ultimately, this sequence of events leads to cell death by apoptosis
702 (Bakkali et al., 2008). Different sized MCM-41 and SBA-15 microparticles induce ROS
703 formation, especially O_2^-, at concentrations over 1 mg/mL after 3 h of incubation on Caco-
704 2 cells, which overwhelms antioxidant defences, causes mitochondrial dysfunction and
705 increases apoptotic signalling (Heikkilä et al., 2010). As found herein for the EOCs-
706 functionalised silica, metabolic activity is a more sensitive endpoint, as measured by ATP
707 depletion, than cell membrane integrity (Heikkilä et al., 2010). However, both the bare
708 MCM-41 microparticles and EOCs exhibited cytotoxic effects and ROS generation at
709 much higher concentrations that those found for the functionalised particles, which are
710 the object of this study. Our results suggest that either a synergistic effect given the
711 presence of both silanol groups from the bulk material and EOCs derivatives from the
712 functionalisation process on the functionalised particles surface or a boosting effect of
713 EOCs as a consequence of their higher density or reduced volatility increased EOCs-cell
714 membrane interactions (Fuentes et al., 2021). Another possible explanation is that EOCs
715 in their free form can be partly metabolised by cells and this phenomenon is not possible
716 for immobilised compounds. Nonetheless, the cellular uptake of microparticles by HepG2
717 cells would still need to be dismissed by confocal microscopy analyses in the future.

718 Alternatives to synthetic preservatives for food applications are not free of potential
719 toxicological hazards. As observed in this work, toxicity studies are necessary to
720 understand the interactions of new materials with biological systems and to guarantee

their safety for human health. In summary, our results show that the functionalisation of silica MCM-41 microparticles with natural EOCs carvacrol and thymol increased these materials' cytotoxic potential compared to their free constituents. Both particle types behaved similarly as regards their cytotoxic effects, which emerged from microparticles themselves, and not from the degradation products released to culture media. The results found in this study generally support the hypothesis that the carvacrol- and thymol-functionalised MCM-41 induce toxicity on HepG2 cells by an oxidative stress-related mechanism. A direct physical interaction between the particles surface and cell membranes could be responsible for inducing ROS overproduction. Oxidative stress would lead to the oxidation of different cellular components like lipids, and also to $\Delta\Psi m$ function that would, in turn, trigger apoptosis signalling through the mitochondrial pathway, and would ultimately lead to cell death by both the proteolytic cascade of pro-apoptotic enzymes and the damage caused to the mitochondrial function. These results should be considered when designing new hybrid materials for food-industry applications.

Acknowledgements

The authors gratefully acknowledge the financial support from the Spanish government (Project RTI2018-101599-B-C21 (MCUI/AEI/FEDER, EU)).

References

Abbasi, F., Hashemi, H., Samaei, M.R., SavarDashtaki, A., Azhdarpoor, A., Fallahi, M.J., 2021. The synergistic interference effect of silica nanoparticles concentration and the wavelength of ELISA on the colorimetric assay of cell toxicity. Sci. Rep. 11,

15133. https://doi.org/10.1038/s41598-021-92419-1

Abbaszadeh, S., Sharifzadeh, A., Shokri, H., Khosravi, A.R., Abbaszadeh, A., 2014. Antifungal efficacy of thymol, carvacrol, eugenol and menthol as alternative agents to control the growth of food-relevant fungi. J. Mycol. Med. 24, 51–56. https://doi.org/10.1016/J.MYCMED.2014.01.063

Abdelhamid, A.G., Yousef, A.E., 2021. Natural Antimicrobials Suitable for Combating Desiccation-Resistant Salmonella enterica in Milk Powder. Microorg. 2021, Vol. 9, Page 421 9, 421. https://doi.org/10.3390/MICROORGANISMS9020421

Aburawi, E.H., Qureshi, M.A., Oz, D., Jayaprakash, P., Tariq, S., Hameed, R.S., Das, S., Goswami, A., Biradar, A. V., Asefa, T., Souid, A.-K., Adeghate, E., Howarth, F.C., 2012. Biocompatibility of Calcined Mesoporous Silica Particles with Ventricular Myocyte Structure and Function. Chem. Res. Toxicol. 26, 26–36. https://doi.org/10.1021/TX300255U

Al-Salam, S., Balhaj, G., Al-Hammadi, S., Sudhadevi, M., Tariq, S., Biradar, A. V., Asefa, T., Souid, A.-K., 2011. In Vitro Study and Biocompatibility of Calcined Mesoporous Silica Microparticles in Mouse Lung. Toxicol. Sci. 122, 86–99. https://doi.org/10.1093/TOXSCI/KFR078

Alothman, Z., 2012. A Review: Fundamental Aspects of Silicate Mesoporous Materials. Materials (Basel). 5, 2874–2902. https://doi.org/10.3390/ma5122874

Aranda, A., Sequedo, L., Tolosa, L., Quintas, G., Burello, E., Castell, J. V., Gombau, L., 2013. Dichloro-dihydro-fluorescein diacetate (DCFH-DA) assay: A quantitative method for oxidative stress assessment of nanoparticle-treated cells. Toxicol. Vitr. 27, 954–963. https://doi.org/10.1016/j.tiv.2013.01.016

768 Aslantürk, Ö.S., 2018. In Vitro Cytotoxicity and Cell Viability Assays: Principles,
769 Advantages, and Disadvantages, in: Genotoxicity - A Predictable Risk to Our Actual
770 World. InTech. https://doi.org/10.5772/intechopen.71923

771 Bagheri, E., Ansari, L., Abnous, K., Taghdisi, S.M., Charbgoo, F., Ramezani, M.,
772 Alibolandi, M., 2018. Silica based hybrid materials for drug delivery and
773 bioimaging. J. Control. Release. https://doi.org/10.1016/j.jconrel.2018.03.014

774 Bakkali, F., Averbeck, S., Averbeck, D., Idaomar, M., 2008. Biological effects of
775 essential oils – A review. Food Chem. Toxicol. 46, 446–475.
776 https://doi.org/10.1016/j.fct.2007.09.106

777 Barrera, G., 2012. Oxidative Stress and Lipid Peroxidation Products in Cancer
778 Progression and Therapy. ISRN Oncol. 2012, 1–21.
779 https://doi.org/10.5402/2012/137289

780 Boelsterli, U.A., 2007. Mechanistic toxicology : the molecular basis of how chemicals
781 disrupt biological targets. CRC Press.

782 Burt, S., 2004. Essential oils: their antibacterial properties and potential applications in
783 foods—a review. Int. J. Food Microbiol. 94, 223–253.
784 https://doi.org/10.1016/J.IJFOODMICRO.2004.03.022

785 Čabarkapa, I., Čolović, R., Đuragić, O., Popović, S., Kokić, B., Milanov, D., Pezo, L.,
786 2019. Anti-biofilm activities of essential oils rich in carvacrol and thymol against
787 Salmonella Enteritidis. https://doi.org/10.1080/08927014.2019.1610169 35, 361–
788 375. https://doi.org/10.1080/08927014.2019.1610169

789 Cabrera, S., El Haskouri, J., Guillem, C., Latorre, J., Beltrán-Porter, A., Beltrán-Porter,
790 D., Marcos, M.D., Amorós, P., 2000. Generalised syntheses of ordered mesoporous

oxides: The atrane route. Solid State Sci. 2, 405–420. https://doi.org/10.1016/S1293-2558(00)00152-7

Casey, A., Herzog, E., Lyng, F.M., Byrne, H.J., Chambers, G., Davoren, M., 2008. Single walled carbon nanotubes induce indirect cytotoxicity by medium depletion in A549 lung cells. Toxicol. Lett. 179, 78–84. https://doi.org/10.1016/J.TOXLET.2008.04.006

Chen, F., Shi, Z., Neoh, K.G., Kang, E.T., 2009. Antioxidant and antibacterial activities of eugenol and carvacrol-grafted chitosan nanoparticles. Biotechnol. Bioeng. 104, 30–39. https://doi.org/10.1002/bit.22363

Ciappellano, S.G., Tedesco, E., Venturini, M., Benetti, F., 2016. In vitro toxicity assessment of oral nanocarriers. Adv. Drug Deliv. Rev. https://doi.org/10.1016/j.addr.2016.08.007

D'Arcy, M.S., 2019. Cell death: a review of the major forms of apoptosis, necrosis and autophagy. Cell Biol. Int. 43, 582–592. https://doi.org/10.1002/CBIN.11137

Diab, R., Canilho, N., Pavel, I.A., Haffner, F.B., Girardon, M., Pasc, A., 2017. Silica-based systems for oral delivery of drugs, macromolecules and cells. Adv. Colloid Interface Sci. 249, 346–362. https://doi.org/10.1016/j.cis.2017.04.005

Dumitrescu, E., Karunaratne, D.P., Prochaska, M.K., Liu, X., Wallace, K.N., Andreescu, S., 2017. Developmental toxicity of glycine-coated silica nanoparticles in embryonic zebrafish. Environ. Pollut. 229, 439–447. https://doi.org/10.1016/J.ENVPOL.2017.06.016

Eisenbrand, G., Pool-Zobel, B., Baker, V., Balls, M., Blaauboer, B.J., Boobis, A., Carere, A., Kevekordes, S., Lhuguenot, J.C., Pieters, R., Kleiner, J., 2002. Methods of in

vitro toxicology. Food Chem. Toxicol. https://doi.org/10.1016/S0278-6915(01)00118-1

Faleiro, M.L., Miguel, G., 2020. Antimicrobial and Antioxidant Activities of Natural Compounds: Enhance the Safety and Quality of Food. Foods 2020, Vol. 9, Page 1145 9, 1145. https://doi.org/10.3390/FOODS9091145

Ferrer, E., Juan-García, A., Font, G., Ruiz, M.J., 2009. Reactive oxygen species induced by beauvericin, patulin and zearalenone in CHO-K1 cells. Toxicol. Vitr. 23, 1504–1509. https://doi.org/10.1016/j.tiv.2009.07.009

Fotakis, G., Timbrell, J.A., 2006. In vitro cytotoxicity assays: Comparison of LDH, neutral red, MTT and protein assay in hepatoma cell lines following exposure to cadmium chloride. Toxicol. Lett. 160, 171–177. https://doi.org/10.1016/J.TOXLET.2005.07.001

Fuentes, C., Ruiz-Rico, M., Fuentes, A., Barat, J.M., Ruiz, M.J., 2021. Comparative cytotoxic study of silica materials functionalised with essential oil components in HepG2 cells. Food Chem. Toxicol. 147, 111858. https://doi.org/10.1016/j.fct.2020.111858

Fuentes, C., Ruiz-Rico, M., Fuentes, A., Ruiz, M.J., Barat, J.M., 2020. Degradation of silica particles functionalised with essential oil components under simulated physiological conditions. J. Hazard. Mater. 399, 123120. https://doi.org/10.1016/j.jhazmat.2020.123120

García-Ríos, E., Ruiz-Rico, M., Guillamón, J.M., Pérez-Esteve, É., Barat, J.M., 2018. Improved antimicrobial activity of immobilised essential oil components against representative spoilage wine microorganisms. Food Control 94, 177–186. https://doi.org/10.1016/j.foodcont.2018.07.005

838 Garrido-Cano, I., Candela-Noguera, V., Herrera, G., Cejalvo, J.M., Lluch, A., Marcos,
839 M.D., Sancenon, F., Eroles, P., Martínez-Máñez, R., 2021. Biocompatibility and
840 internalization assessment of bare and functionalised mesoporous silica
841 nanoparticles. Microporous Mesoporous Mater. 310, 110593.
842 https://doi.org/10.1016/J.MICROMESO.2020.110593

843 Hamilton, R.F., Thakur, S.A., Holian, A., 2008. Silica binding and toxicity in alveolar
844 macrophages. Free Radic. Biol. Med. 44, 1246–1258.
845 https://doi.org/10.1016/j.freeradbiomed.2007.12.027

846 Heikkilä, T., Santos, H.A., Kumar, N., Murzin, D.Y., Salonen, J., Laaksonen, T.,
847 Peltonen, L., Hirvonen, J., Lehto, V.-P., 2010. Cytotoxicity study of ordered
848 mesoporous silica MCM-41 and SBA-15 microparticles on Caco-2 cells. Eur. J.
849 Pharm. Biopharm. 74, 483–494. https://doi.org/10.1016/J.EJPB.2009.12.006

850 Herzog, E., Byrne, H.J., Davoren, M., Casey, A., Duschl, A., Oostingh, G.J., 2009.
851 Dispersion medium modulates oxidative stress response of human lung epithelial
852 cells upon exposure to carbon nanomaterial samples. Toxicol. Appl. Pharmacol. 236,
853 276–281. https://doi.org/10.1016/J.TAAP.2009.02.007

854 Holder, A.L., Goth-Goldstein, R., Lucas, D., Koshland, C.P., 2012. Particle-Induced
855 Artifacts in the MTT and LDH Viability Assays. https://doi.org/10.1021/tx3001708

856 Hyldgaard, M., Mygind, T., Meyer, R.L., 2012. Essential oils in food preservation: Mode
857 of action, synergies, and interactions with food matrix components. Front.
858 Microbiol. 3, 1–12. https://doi.org/10.3389/fmicb.2012.00012

859 Jeong, S.Y., Seol, D.W., 2008. The role of mitochondria in apoptosis. J. Biochem. Mol.
860 Biol. https://doi.org/10.5483/bmbrep.2008.41.1.011

Karam, L., Roustom, R., Abiad, M.G., El-Obeid, T., Savvaidis, I.N., 2019. Combined effects of thymol, carvacrol and packaging on the shelf-life of marinated chicken. Int. J. Food Microbiol. 291, 42–47. https://doi.org/10.1016/J.IJFOODMICRO.2018.11.008

Korhonen, E., Rönkkö, S., Hillebrand, S., Riikonen, J., Xu, W., Järvinen, K., Lehto, V.P., Kauppinen, A., 2016. Cytotoxicity assessment of porous silicon microparticles for ocular drug delivery. Eur. J. Pharm. Biopharm. 100, 1–8. https://doi.org/10.1016/J.EJPB.2015.11.020

Kroll, A., Pillukat, M.H., Hahn, D., Schnekenburger, J., 2012. Interference of engineered nanoparticles with in vitro toxicity assays. Arch. Toxicol. 86, 1123–1136. https://doi.org/10.1007/s00204-012-0837-z

Kyriakidou, K., Brasinika, D., Trompeta, A.F.A., Bergamaschi, E., Karoussis, I.K., Charitidis, C.A., 2020. In vitro cytotoxicity assessment of pristine and carboxyl-functionalized MWCNTs. Food Chem. Toxicol. 141, 111374. https://doi.org/10.1016/j.fct.2020.111374

Laaksonen, T., Santos, H., Vihola, H., Salonen, J., Riikonen, J., Heikkilä, T., Peltonen, L., Kumar, N., Murzin, D.Y., Lehto, V.P., Hirvonen, J., 2007. Failure of MTT as a toxicity testing agent for mesoporous silicon microparticles. Chem. Res. Toxicol. 20, 1913–1918. https://doi.org/10.1021/tx700326b

Lehman, S.E., Morris, A.S., Mueller, P.S., Salem, A.K., Grassian, V.H., Larsen, S.C., 2016. Silica nanoparticle-generated ROS as a predictor of cellular toxicity: Mechanistic insights and safety by design. Environ. Sci. Nano 3, 56–66. https://doi.org/10.1039/c5en00179j

Meynen, V., Cool, P., Vansant, E.F., 2009. Verified syntheses of mesoporous materials.

885 Microporous Mesoporous Mater. 125, 170–223.
886 https://doi.org/10.1016/J.MICROMESO.2009.03.046

887 Miret, S., De Groene, E.M., Klaffke, W., 2006. Comparison of in vitro assays of cellular
888 toxicity in the human hepatic cell line HepG2. J. Biomol. Screen. 11, 184–193.
889 https://doi.org/10.1177/1087057105283787

890 Paatero, I., Casals, E., Niemi, R., Özliseli, E., Rosenholm, J.M., Sahlgren, C., 2017.
891 Analyses in zebrafish embryos reveal that nanotoxicity profiles are dependent on
892 surface-functionalization controlled penetrance of biological membranes. Sci. Rep.
893 7. https://doi.org/10.1038/S41598-017-09312-Z

894 Peña-Gómez, N., Ruiz-Rico, M., Fernández-Segovia, I., Barat, J.M., 2019a. Study of
895 apple juice preservation by filtration through silica microparticles functionalised
896 with essential oil components. Food Control 106, 106749.
897 https://doi.org/10.1016/j.foodcont.2019.106749

898 Peña-Gómez, N., Ruiz-Rico, M., Pérez-Esteve, É., Fernández-Segovia, I., Barat, J.M.,
899 2020. Microbial stabilization of craft beer by filtration through silica supports
900 functionalized with essential oil components. LWT 117, 108626.
901 https://doi.org/10.1016/j.lwt.2019.108626

902 Peña-Gómez, N., Ruiz-Rico, M., Pérez-Esteve, É., Fernández-Segovia, I., Barat, J.M.,
903 2019b. Novel antimicrobial filtering materials based on carvacrol, eugenol, thymol
904 and vanillin immobilized on silica microparticles for water treatment. Innov. Food
905 Sci. Emerg. Technol. 58, 102228. https://doi.org/10.1016/j.ifset.2019.102228

906 Puerari, R.C., Ferrari, E., de Cezar, M.G., Gonçalves, R.A., Simioni, C., Ouriques, L.C.,
907 Vicentini, D.S., Matias, W.G., 2019. Investigation of toxicological effects of
908 amorphous silica nanostructures with amine-functionalized surfaces on Vero cells.

Chemosphere 214, 679–687. https://doi.org/10.1016/j.chemosphere.2018.09.165

Puerari, R.C., Ferrari, E., Oscar, B.V., Simioni, C., Ouriques, L.C., Vicentini, D.S., Matias, W.G., 2021. Acute and chronic toxicity of amine-functionalized SiO2 nanostructures toward Daphnia magna. Ecotoxicol. Environ. Saf. 212, 111979. https://doi.org/10.1016/J.ECOENV.2021.111979

Ray, P.D., Huang, B.-W., Tsuji, Y., 2012. Reactive oxygen species (ROS) homeostasis and redox regulation in cellular signaling. Cell. Signal. 24, 981. https://doi.org/10.1016/J.CELLSIG.2012.01.008

Ribes, S., Fuentes, A., Talens, P., Barat, J.M., 2018. Prevention of fungal spoilage in food products using natural compounds: A review. Crit. Rev. Food Sci. Nutr. 58, 2002–2016. https://doi.org/10.1080/10408398.2017.1295017

Ribes, S., Ruiz-Rico, M., Pérez-Esteve, É., Fuentes, A., Barat, J.M., 2019. Enhancing the antimicrobial activity of eugenol, carvacrol and vanillin immobilised on silica supports against Escherichia coli or Zygosaccharomyces rouxii in fruit juices by their binary combinations. LWT 113, 108326. https://doi.org/10.1016/j.lwt.2019.108326

Ribes, S., Ruiz-Rico, M., Pérez-Esteve, É., Fuentes, A., Talens, P., Martínez-Máñez, R., Barat, J.M., 2017. Eugenol and thymol immobilised on mesoporous silica-based material as an innovative antifungal system: Application in strawberry jam. Food Control 81, 181–188. https://doi.org/10.1016/J.FOODCONT.2017.06.006

Ros-Lis, J. V., Bernardos, A., Pérez, É., Barat, J.M., Martínez-Máñez, R., 2018. Functionalized Silica Nanomaterials as a New Tool for New Industrial Applications, in: Impact of Nanoscience in the Food Industry. Elsevier Inc., pp. 165–196. https://doi.org/10.1016/B978-0-12-811441-4.00007-8

933 Ruiz-Leal, M., George, S., 2004. An in vitro procedure for evaluation of early stage
934 oxidative stress in an established fish cell line applied to investigation of PHAH and
935 pesticide toxicity. Mar. Environ. Res. 58, 631–635.
936 https://doi.org/10.1016/J.MARENVRES.2004.03.054

937 Saei, A.A., Yazdani, M., Lohse, S.E., Bakhtiary, Z., Serpooshan, V., Ghavami, M.,
938 Asadian, M., Mashaghi, S., Dreaden, E.C., Mashaghi, A., Mahmoudi, M., 2017.
939 Nanoparticle Surface Functionality Dictates Cellular and Systemic Toxicity. Chem.
940 Mater. 29, 6578–6595. https://doi.org/10.1021/ACS.CHEMMATER.7B01979

941 Samri, M.T. Al, Biradar, A. V, Alsuwaidi, A.R., Balhaj, G., Al-Hammadi, S., Shehab, S.,
942 Al-Salam, S., Tariq, S., Pramathan, T., Benedict, S., Asefa, T., Souid, A.-K., 2012.
943 In vitro biocompatibility of calcined mesoporous silica particles and fetal blood
944 cells. Int. J. Nanomedicine 7, 3111. https://doi.org/10.2147/IJN.S32711

945 Santos, H.A., Riikonen, J., Salonen, J., Mäkilä, E., Heikkilä, T., Laaksonen, T., Peltonen,
946 L., Lehto, V.-P., Hirvonen, J., 2010. In vitro cytotoxicity of porous silicon
947 microparticles: Effect of the particle concentration, surface chemistry and size. Acta
948 Biomater. 6, 2721–2731. https://doi.org/10.1016/J.ACTBIO.2009.12.043

949 Severin, I., Souton, E., Dahbi, L., Chagnon, M.C., 2017. Use of bioassays to assess hazard
950 of food contact material extracts: State of the art. Food Chem. Toxicol. 105, 429–
951 447. https://doi.org/10.1016/J.FCT.2017.04.046

952 Shamsi, M. Al, Samri, M.T. Al, Al-Salam, S., Conca, W., Shaban, S., Benedict, S., Tariq,
953 S., Biradar, A. V., Penefsky, H.S., Asefa, T., Souid, A.-K., 2010. Biocompatibility
954 of Calcined Mesoporous Silica Particles with Cellular Bioenergetics in Murine
955 Tissues. Chem. Res. Toxicol. 23, 1796–1805. https://doi.org/10.1021/TX100245J

956 Tait, S.W.G., Green, D.R., 2013. Mitochondrial regulation of cell death. Cold Spring

957 Harb. Perspect. Biol. 5, a008706. https://doi.org/10.1101/cshperspect.a008706

958 Tippayatum, P., Chonhenchob, V., 2007. Antibacterial activities of thymol, eugenol and
959 nisin against some food spoilage bacteria. Nat. Sci. 41, 319–23.

960 Vicentini, D.S., Puerari, R.C., Oliveira, K.G., Arl, M., Melegari, S.P., Matias, W.G.,
961 2017. Toxicological impact of morphology and surface functionalization of
962 amorphous SiO2 nanomaterials. NanoImpact 5, 6–12.
963 https://doi.org/10.1016/J.IMPACT.2016.11.003

964 Walczak, M., Michalska-Sionkowska, M., Olkiewicz, D., Tarnawska, P., Warżyńska, O.,
965 2021. Potential of Carvacrol and Thymol in Reducing Biofilm Formation on
966 Technical Surfaces. Mol. 2021, Vol. 26, Page 2723 26, 2723.
967 https://doi.org/10.3390/MOLECULES26092723

968 Wang, C., Youle, R.J., 2009. The Role of Mitochondria in Apoptosis. Annu. Rev. Genet.
969 43, 95. https://doi.org/10.1146/ANNUREV-GENET-102108-134850

970 Weyermann, J., Lochmann, D., Zimmer, A., 2005. A practical note on the use of
971 cytotoxicity assays. Int. J. Pharm. 288, 369–376.
972 https://doi.org/10.1016/J.IJPHARM.2004.09.018

973 Xu, J., Zhou, F., Ji, B.P., Pei, R.S., Xu, N., 2008. The antibacterial mechanism of
974 carvacrol and thymol against Escherichia coli. Lett. Appl. Microbiol. 47, 174–179.
975 https://doi.org/10.1111/j.1472-765X.2008.02407.x

976 Xu, J.J., Diaz, D., O'Brien, P.J., 2004. Applications of cytotoxicity assays and pre-lethal
977 mechanistic assays for assessment of human hepatotoxicity potential. Chem. Biol.
978 Interact. 150, 115–128. https://doi.org/10.1016/J.CBI.2004.09.011

979 Yu, T., Malugin, A., Ghandehari, H., 2011. Impact of silica nanoparticle design on

cellular toxicity and hemolytic activity. ACS Nano 5, 5717–5728. https://doi.org/10.1021/NN2013904/SUPPL_FILE/NN2013904_SI_001.PDF

Zhang, Y., 2018. Cell toxicity mechanism and biomarker. Clin. Transl. Med. 7, 34. https://doi.org/10.1186/s40169-018-0212-7